

## Hard underlying event correction to inclusive jet cross sections

Jon Pumplin\*

*Department of Physics & Astronomy, Michigan State University, East Lansing, Michigan 48824*

(Received 18 August 1997; published 9 April 1998)

Jets observed in hadron-hadron scattering contain a contribution from the “underlying event” that is produced by spectator interactions taking place incoherently with the major parton-parton collision, due to the extended composite structure of the colliding hadrons. Using a recent measurement of the double parton interaction rate, we calculate that the underlying event may be 2–3 times stronger than generally assumed, as a result of semi-hard perturbative multiple-parton interactions. This can have an important influence on the inclusive jet cross section at moderate values of  $E_T$ , persisting at the 5–10 % level to the largest observable  $E_T$ . We show how the underlying event can be measured accurately using a generalization of a method first proposed by Marchesini and Webber. [S0556-2821(98)01311-3]

PACS number(s): 13.87.–a, 12.38.Aw

### I. INTRODUCTION

The inclusive jet cross section  $d\sigma/dE_T$ , averaged over a small range of pseudorapidity, is an important object for study because it tests perturbative QCD at the highest  $Q^2$  scale currently possible [1,2]. Beyond its potential for detecting physics beyond the standard model or confirming QCD, the jet cross section is even beginning to play a role in the global data fitting used to measure parton distribution functions [3,4]. It is therefore important to carefully consider all systematic effects that influence the interpretation of the measurement.

Among those effects is the “underlying event” generated by spectator interactions that can occur concurrently with a major parton-parton collision, due to the extended composite structure of the colliding hadrons. Simulations such as the HERWIG Monte Carlo [5] program include a “soft” underlying event that is modeled by a parametrization of minimum bias data.<sup>1</sup> However, there may also be a *hard* underlying event: particles can be created by incoherent parton-parton interactions at momentum transfers that are sufficiently large for perturbative QCD to be a useful approximation, but much smaller than that of the interaction mainly responsible for a given high  $E_T$  jet event.

Attempts have been made in the past to predict underlying event contributions, including the perturbative part that is the focus of our attention [7–9]. We make a new estimate here, based on a recent direct measurement [10] of the rate for double parton interactions in hard scattering. In the following sections we derive the prediction, show how it can be independently tested by experiment, and discuss its effect on the inclusive cross section.

### II. HARD UNDERLYING EVENT

To generate typical semi-hard perturbative final states, HERWIG [5] was used to simulate QCD  $2 \rightarrow 2$  hard scattering at the Tevatron energy  $\sqrt{s} = 1.8$  TeV, with the minimum  $p_\perp$  parameter for the hard scattering set to a fairly small value (PTMIN = 2.0 GeV) that is nevertheless large enough for comfort with the perturbative calculation. This choice yields a cross section  $\sigma = 50.6$  mb, which is about equal to the full inelastic non-diffractive cross section ( $50.9 \pm 1.5$  mb) [11]; so we appear to be taking an extreme point of view in which that cross section is mainly generated by perturbative (“minijet”) interactions. The point of view is actually not so extreme, since including  $s$ -channel unitarity effects, e.g., by an eikonal model, would substantially reduce the cross section on the basis that once one interaction has taken place, additional interactions do not really add to the inelastic cross section [12,13]. The soft underlying event feature of HERWIG was turned off (PRSOFF = 0), since our goal is to study the perturbative part of the underlying event.

If  $\sigma_1$  and  $\sigma_2$  are cross sections for distinguishable rare parton-parton interactions, the cross section for both interactions to occur in the same event can be written as

$$\sigma_{\text{double}} = \frac{\sigma_1 \sigma_2}{\sigma_{\text{eff}}}, \quad (1)$$

with the parameter  $\sigma_{\text{eff}}$  conveying the probability for double parton interaction.  $\sigma_{\text{eff}}$  carries nonperturbative information beyond the scope of ordinary parton distribution functions, since it relates to correlations between partons within a single hadron. It has recently been measured to be  $\sigma_{\text{eff}} = 14.5 \pm 1.7 \pm_{2,3}^{1.7}$  mb [10].

For a fixed small value of  $\sigma_1$ , corresponding to some rare hard scattering of type 1, Eq. (1) gives  $\sigma_2/\sigma_{\text{eff}}$  as the probability for a second rare scattering of type 2. If this type 2 scattering is not rare, and it occurs randomly, the obvious generalization of Eq. (1) is a Poisson distribution in the number  $n$  of type 2 interactions that accompany a given type 1 interaction:

\*Email address (internet): pumplin@pa.msu.edu

<sup>1</sup>Minimum bias events provide at best an imperfect model of the underlying event, since for example they always contain particles; while the soft underlying event can sometimes be absent, as shown by the finite survival probability for inelastic events with large rapidity gaps [6].

$$P_n = \frac{a^n}{n!} e^{-a} \quad (2)$$

with mean number  $a = \sigma_2 / \sigma_{\text{eff}}$ .

Our model for the hard underlying event therefore consists of superimposing  $n$  of the above minijet events from HERWIG, with a Poisson probability distribution (2) of mean  $a = 50.6 \text{ mb} / 14.5 \text{ mb} = 3.49$ . In doing this, we ignore energy-momentum conservation effects in the sense that the parton momentum distributions are taken to be the same as in single-interaction events. This assumption should be adequate because the minijet interactions do not require a great deal of energy, and thus come from partons at rather small  $x$ . (More elaborate models [7,8] based on PYTHIA [14], and [9] based on HERWIG, have incorporated these energy-momentum constraints.) Meanwhile, the Poisson assumption could actually *underestimate* the frequency of 3 or more interactions, since these may be enhanced by ‘‘hot spots’’ — e.g., by strong spatial correlations between the partons in a beam or target hadron associated with constituent quarks [15].

In this paper, we focus specifically on the case of the underlying event in dijet production. However, it will be valuable to look also at  $W$ ,  $Z^0$ , or lepton pair production, where the hard scattering makes a color-neutral object, so there is no radiation associated with final state jets. These processes also share the advantage that the hard scattering is initiated by  $q\bar{q}$ , which generates less radiation than  $qg$  or  $gg$ . Single jet final states such as  $W+1$  jet and  $\gamma+1$  jet should also be studied.

We generate events with jets of transverse energy  $E_T > 100 \text{ GeV}$  using HERWIG, and look at the total transverse energy inside a control region cone  $R = \sqrt{(\eta - \eta_0)^2 + (\phi - \phi_0)^2} < 0.7$ , which is a size typically used to define jets in the pseudorapidity-azimuthal angle ‘‘Lego’’ plane [1]. The underlying event is by definition uncorrelated with the jets, so to avoid the majority of the jet  $E_T$ , the control cone is centered a distance  $R=2.0$  away from both jet axes, in a manner to be described fully in Sec. III.

Figure 1 shows the distribution of transverse energy  $E_T$  in the control region cone from the HERWIG soft underlying event (dashed curve) and from the hard underlying event model (dotted curve). The average values, which are relevant for the correction to the inclusive jet cross section as will be discussed in Sec. IV, are  $\langle E_T \rangle = 0.84 \text{ GeV}$  for the soft background and  $\langle E_T \rangle = 1.90 \text{ GeV}$  for the hard background. For comparison, Fig. 1 also shows the predicted contribution from radiation associated with the hard scattering (solid curve), as given by HERWIG with the underlying event turned off. It has  $\langle E_T \rangle = 2.37 \text{ GeV}$ .

The hard underlying event model predicts a substantially larger  $\langle E_T \rangle$  than the soft model. Taken as estimates of the average underlying event  $E_T$  that should be added to a perturbative QCD calculation to predict the observed inclusive jet cross section, the difference is significant as will be discussed in Sec. IV — the more so if both mechanisms operate concurrently, so their contributions to  $E_T$  should be added.

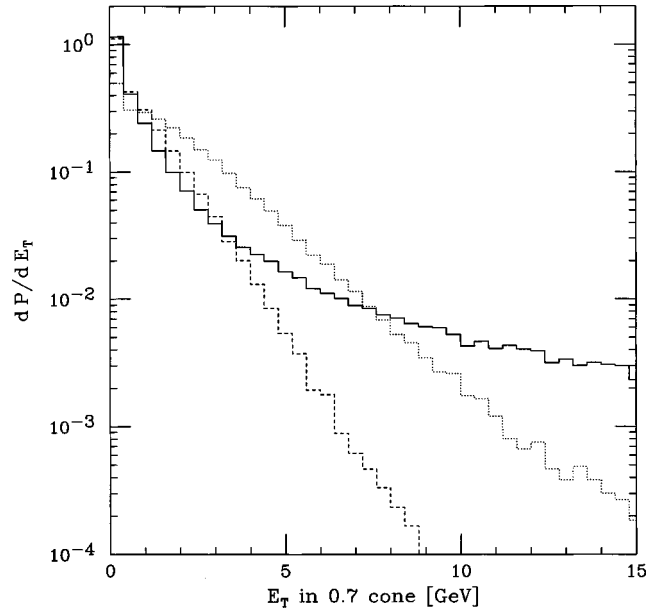


FIG. 1. Normalized probability distributions for  $E_T$  in  $R=0.7$  control cone. Solid curve = HERWIG with soft underlying event off; dashed curve = soft underlying event from HERWIG; dotted curve = hard underlying event from Sec. II.

Before turning to the influence on inclusive jet cross sections, we first consider how to measure the background event better.

### III. OBSERVING THE UNDERLYING EVENT

An obvious way to measure the background event contribution to jets is to look at the  $E_T$  distribution in a ‘‘control region’’ cone of the same radius that is used to identify jets, as discussed in the preceding section. Figure 2 shows the predicted probability distributions, which correspond to adding the contributions described by Fig. 1: HERWIG with its soft underlying event model included (dashed curve), HERWIG with its soft underlying event portion replaced by the hard underlying event model of Sec. II (dotted curve), and HERWIG with both underlying event models operative (solid curve). All three curves share contributions from the substantial QCD radiation generated by the principal hard scattering and its color connections to the beam particles. This makes the curves somewhat similar, but the differences are large enough that a measurement of this control  $E_T$  distribution would give a useful indication of the background event level.

To measure the underlying event more accurately, we generalize a technique first advocated some time ago by Marchesini and Webber [16] — which has apparently not yet been applied in its original form. The essence of the technique is to study  $E_T$  simultaneously in two regions that are separate from each other and separate from any jets that define the final state under study, and to look in particular at the smaller of the two measured  $E_T$ 's.

We describe the proposed generalization in the context of our application to dijet events. Let  $(\eta_1, \phi_1)$  and  $(\eta_2, \phi_2)$  be the locations of the jets in the Lego plane. For this study, we make the approximation that the jets are back-to-back in azimuth:  $|\phi_1 - \phi_2| = \pi$ . Label the jets so that  $\eta_1 < \eta_2$  and let

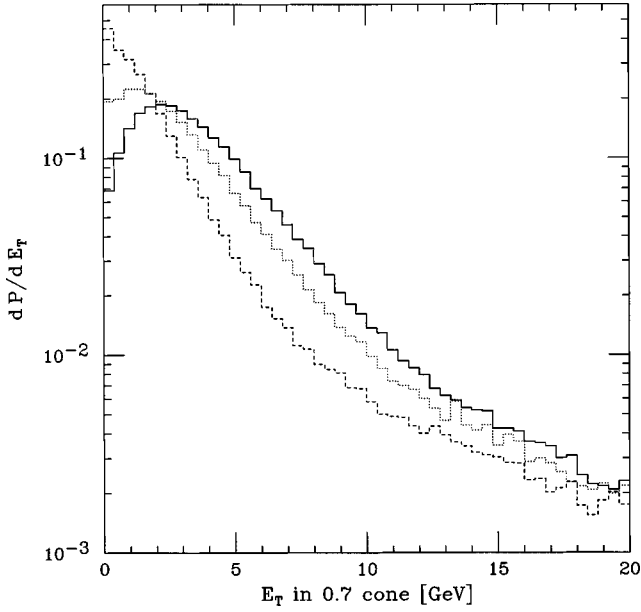


FIG. 2. Predicted probability distributions for  $E_T$  in  $R=0.7$  control cone. Dashed curve = HERWIG including soft underlying event; dotted curve = HERWIG with soft underlying event replaced by hard underlying event model of Sec. II; solid curve = HERWIG with both soft and hard underlying event included.

$$\kappa = \sqrt{4[\pi^2 + (\eta_1 - \eta_2)^2] - 1/4} \quad , \quad (3)$$

rejecting the small fraction (5.6%) of events that have  $|\eta_1 - \eta_2| > 2.48$ , for which  $\kappa$  is undefined. Then consider the two points  $(\eta_a, \phi_a)$  and  $(\eta_b, \phi_b)$  where

$$\eta_a = \eta_b = (\eta_1 + \eta_2)/2 + \kappa\pi \quad (4)$$

$$\phi_{a,b} = \phi_1 \pm (\pi/2 - \kappa|\eta_1 - \eta_2|) \quad . \quad (5)$$

These points are at the same pseudorapidity  $\eta_a = \eta_b$ , and are well separated from each other in azimuth by  $|\phi_a - \phi_b| = \pi - 2\kappa|\eta_1 - \eta_2|$  which varies from 2.28 to 3.14. Both points are separated from both of the jet axes by a distance of exactly 2.0 in the Lego plane. (The jet that lies farther from them in  $\eta$  is therefore closer to them in  $\phi$ .) We can define a similar pair of points by letting  $\kappa \rightarrow -\kappa$  in Eq. (4) and  $\phi_1$

$\rightarrow \phi_2$  in Eq. (5). For the present purpose, we use only the pair of points with  $\eta_a = \eta_b$  closer to  $\eta = 0$  to reduce any kinematic suppression.

Let  $S_a$  and  $S_b$  denote the total transverse energy  $E_T$  deposited in cones of radius 0.7 centered on these two points. Figure 3 shows some typical locations of the cones with respect to the jet axes. From the HERWIG simulation (taking the jet axes from the directions of their partons, without modification by initial state radiation for simplicity), we find  $0 \pm 0.64$  for the mean and standard deviation in  $\eta$  and  $2.59 \pm 0.26$  for the mean and standard deviation in  $|\phi_a - \phi_b|$ . (In practice, it may be better to keep the control cones centered at fixed values of  $\eta$ , at the expense of letting their distances from the jets vary somewhat, to avoid effects due to the  $\eta$ -dependence of detector corrections.)

The cones  $a$  and  $b$  are those already used in Sec. II to study the underlying event background. The two cones are equivalent, and only one was used for each event. Figure 2 can therefore be interpreted as the probability distribution for  $S_a$  or equivalently for  $S_b$ .

Because there is no intrinsic difference between the two control cones, averaging over events would give  $\langle S_a \rangle = \langle S_b \rangle$ . It follows that

$$\langle S_a \rangle = \langle S_b \rangle = \left\langle \frac{S_a + S_b}{2} \right\rangle = \langle S_{\text{diff}} \rangle + \langle S_{\text{min}} \rangle \quad (6)$$

where

$$S_{\text{diff}} = |S_a - S_b|/2 \quad (7)$$

$$S_{\text{min}} = \min(S_a, S_b) \quad . \quad (8)$$

This separation into  $S_{\text{diff}}$  and  $S_{\text{min}}$  is useful, as pointed out in Ref. [16], because next-to-leading order perturbative corrections to the principal hard scattering contribute in at most one of the two regions, and hence contribute only to  $S_{\text{diff}}$ ; while the underlying event (like minimum bias events [17]) is expected to have positive correlations over long distances in  $(\eta, \phi)$ , so its contribution to  $S_{\text{diff}}$  is suppressed while its contribution to  $S_{\text{min}}$  is strong. Thus measuring the distributions of  $S_{\text{diff}}$  and  $S_{\text{min}}$  separately will be much more revealing than the distribution of  $S_a$  or  $S_b$  of Fig. 2 alone.

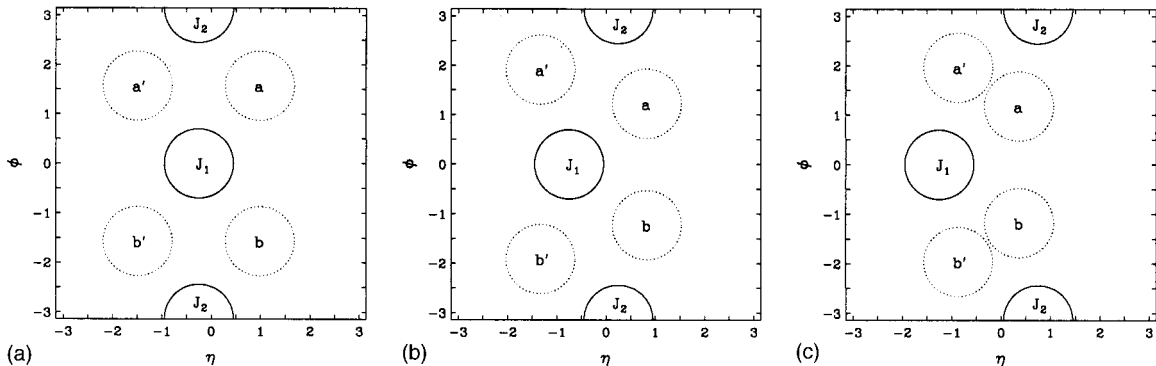


FIG. 3. Typical “control” regions  $a, b, a', b'$  for measuring the transverse energies  $S_a$  and  $S_b$ . Configurations shown are for jets  $J_1$  and  $J_2$  with  $|\eta_1 - \eta_2| = 0.0, 1.0, 2.0$ . The centers of the control regions are a distance 2.0 from both jet axes. The distance from  $a$  to  $b$  is the same as the distance from  $a'$  to  $b'$ , although this is not apparent because the azimuthal cylinder is cut for display at  $|\phi| = \pi$ . We use the pair  $ab$  or  $a'b'$  (here  $ab$ ) that is closer to  $\eta = 0$ .

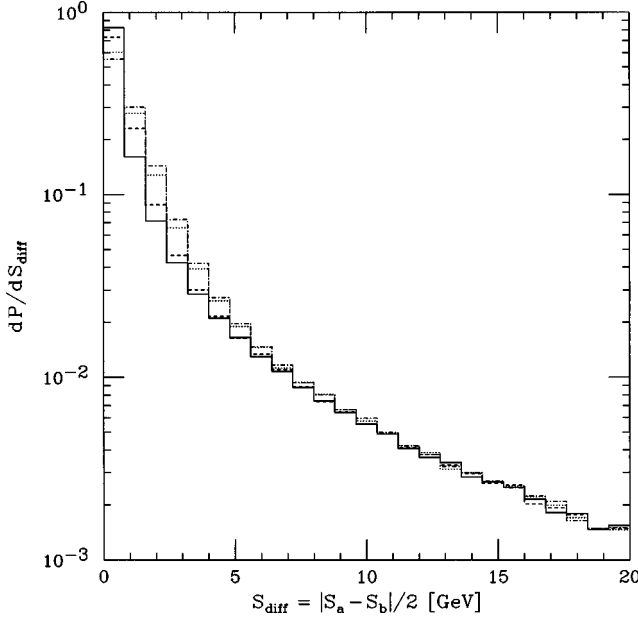


FIG. 4. Normalized probability distributions for  $S_{\text{diff}} = |S_a - S_b|/2$ , where  $S_a$  and  $S_b$  are the total transverse energies in the two  $R=0.7$  control regions. Solid curve = HERWIG with soft underlying event off; dashed curve = HERWIG with soft underlying event on; dotted curve = HERWIG with soft underlying event replaced by hard underlying event from Sec. II; dot-dash curve = HERWIG with both soft and hard underlying event.

Figure 4 shows the predicted probability distributions for  $S_{\text{diff}}$ . As anticipated above,  $S_{\text{diff}}$  is not very sensitive to the choice of model for the underlying event. Testing this distribution against experiment would therefore be a good way to test QCD in a manner that is not very sensitive to underlying event effects.

Figure 5 shows predicted probability distributions for  $S_{\text{min}}$ . As anticipated above,  $S_{\text{min}}$  is *very* sensitive to the underlying event model. Testing this distribution against experiment would therefore be an excellent way to measure the strength of the underlying event.

The method of Marchesini and Webber [16] could be generalized further in the hunt for the background. For example, the transverse energy could be measured in all four of the control regions that can be defined by  $R=0.7$  cones centered 2.0 units in  $(\eta, \phi)$  from both jets. These regions are shown in Fig. 3 for jets that are back-to-back in  $\phi$ . The distribution of the minimum of the four transverse energies, or the distribution of the sum of the two smaller ones, would be especially sensitive to the underlying event. Other cone sizes would also be of interest, but  $R=0.7$  applies most directly to the correction to the inclusive jet cross section.

#### IV. CORRECTION TO $p$ QCD INCLUSIVE JET CROSS SECTION

The influence of the underlying event on the inclusive jet cross section is calculated as follows. Let

$$F(E_T) \equiv \frac{d \sigma_{\text{single}}}{d E_T} \quad (9)$$

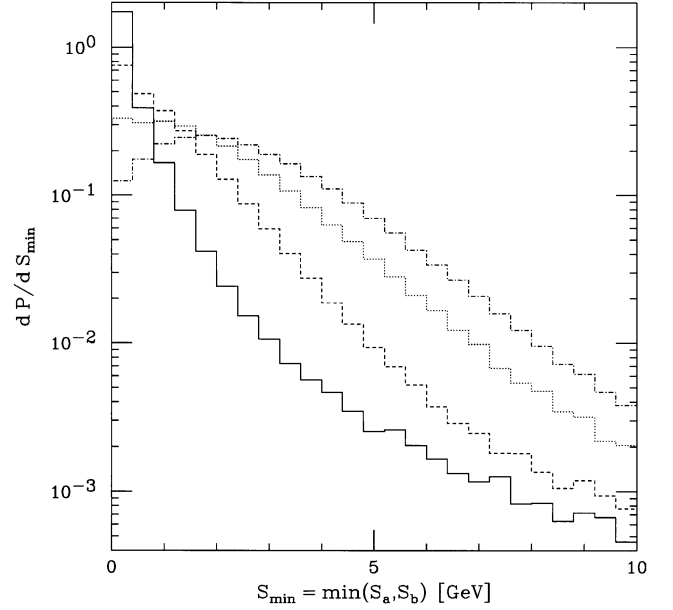


FIG. 5. Normalized probability distributions for  $S_{\text{min}} = \min(S_a, S_b)$ . As in Fig. 4, solid curve = HERWIG with soft underlying event off; dashed curve = HERWIG with soft underlying event on; dotted curve = HERWIG with soft underlying event replaced by hard underlying event from Sec. II; dot-dash curve = HERWIG with both soft and hard underlying event.

be the single hard scattering contribution to the jet cross section, which is predicted by standard perturbative QCD ( $p$ QCD) techniques on the basis of parton distribution functions [3]. Let

$$G(E_T) \equiv \frac{d P}{d E_T} \quad (10)$$

be the probability distribution for additional  $E_T$  inside the jet cone contributed by the underlying event, normalized to  $\int_0^\infty G(E) dE = 1$ . The observable jet  $E_T$  is the total of the two contributions, so the observable inclusive cross section is given by

$$\begin{aligned} F_{\text{obs}}(E_T) &\equiv \frac{d \sigma_{\text{obs}}}{d E_T} = \int_0^\infty dE_1 G(E_1) \int_0^\infty dE_2 F(E_2) \\ &\quad \times \delta(E_1 + E_2 - E_T) \\ &= \int_0^{E_T} G(E_1) F(E_T - E_1) dE_1. \end{aligned} \quad (11)$$

It is assumed here that the underlying event contribution is small enough not to significantly shift the apparent jet axis. In practice there would be a small additional increase in the average jet energy due to the jet-finding algorithm's tendency to maximize the  $E_T$  included in the jet.

Figure 6 shows the fractional increase in the inclusive jet cross section caused by the soft background event (dashed curve); by the hard underlying event model of Sec. II (dotted curve); or by including both underlying event models (dot-dash curve). The effect of the underlying event is rather large

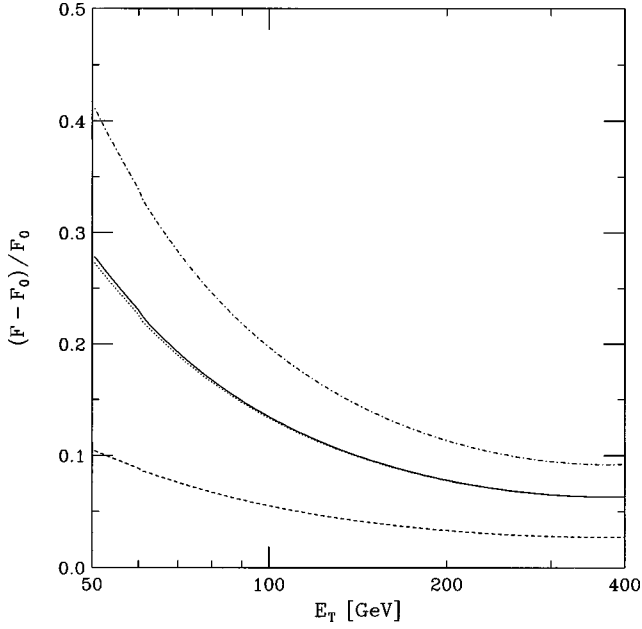


FIG. 6. Fractional increase in the inclusive jet cross section produced by adding HERWIG soft underlying event (dashed curve); the hard underlying event model of Sec. II (dotted curve); or both underlying event contributions (dot-dash curve) to the pQCD prediction. The fractional increase produced above the soft+pQCD prediction by adding the hard underlying event is shown by the solid curve.

at the lower values of jet  $E_T$ , so it must be measured rather well before a meaningful comparison can be made between the observed jet cross section and the pQCD prediction. The effect of the underlying event is significant even at the highest jet  $E_T$  shown, where the cross section is raised by approximately 3%, 6%, or 9% under these three assumptions. The fractional increase caused by adding the hard underlying event to the prediction with the soft underlying event already included is shown by the solid curve in Fig. 6. It is nearly identical to the increase caused by adding it to the pQCD prediction alone (dotted curve).

The procedure used by experimenters [1,2] to take account of the underlying event, along with background from simultaneous events (“pile-up”), is to subtract a constant value from each measured jet  $E_T$ . We examine the accuracy of that approach next.

An average underlying event contribution  $U$  can be defined by the exact equation

$$F_{\text{obs}}(E_T) = F(E_T - U). \quad (12)$$

Since  $G(E)$  falls rapidly with  $E$ , it is natural to make a linear expansion of  $F(E)$  in the neighborhood of  $E_T$  in Eq. (11). The underlying event contribution is then given by

$$U \cong \bar{E} = \int_0^\infty G(E) E dE, \quad (13)$$

which corresponds to the experimental procedure of approximating the background contribution in each event by the average value. This average is subtracted from each measured jet  $E_T$  before obtaining the inclusive cross section that

is compared with pQCD. The value used is 0.9–1.1 GeV, which is similar to the HERWIG soft background prediction  $\langle E_T \rangle = 0.84$  GeV found above. It corresponds to an underlying event level of  $\approx 0.6$ –0.7 GeV per unit area in  $(\eta, \phi)$ .

I find that the linear approximation works rather well for the models considered here, even in the most extreme case where both soft and hard background are included. For example, in that case  $\langle E_T \rangle = 0.84 + 1.90 = 2.74$  GeV, while the true effect corresponds to  $U = 3.0$  for jets of  $E_T = 100$  GeV. However, in real experiments, there is a further background from true minimum bias collisions that occur between other  $p\bar{p}$  pairs at high luminosity. This can easily raise the background level to the point where the linear approximation breaks down. In that case, the collider detector at Fermilab (CDF) analysis method [1] of parametrizing  $F(E_T)$  and fitting the parameters to the experimental results, which is useful to unfold other detector effects anyway, can include this one as well. The essential need is to allow for the event-to-event fluctuations in background.

In the linear approximation, the fractional effect on the inclusive cross section can be written in the form

$$\frac{F_{\text{obs}}(E_T) - F(E_T)}{F(E_T)} \cong \frac{n U}{E_T} \quad (14)$$

where  $n$  is the local effective power law defined by  $F \propto E_T^{-n}$ , i.e.

$$n(E_T) = -d(\ln F)/d(\ln E_T). \quad (15)$$

Over the range  $50 \text{ GeV} < E_T < 400 \text{ GeV}$ ,  $n(E_T)$  rises from  $\approx 5.5$  to  $\approx 12.5$ . Its large value, which represents the rapid fall of the inclusive cross section with  $E_T$ , enhances the effect of the background according to Eq. (14), as has been emphasized recently [18]. For example, it implies that an additional 1–2 GeV of background  $E_T$ , which may be present by the mechanism of Sec. II, will raise the inclusive cross section by 3–6% at  $E_T = 400$  GeV, which is consistent with Fig. 6.

## V. CONCLUSIONS

The point of this paper is that the inclusive jet cross section may contain an underlying event contribution that is 1–2 GeV larger than generally assumed, due to incoherent multiple semi-hard interactions that accompany the hard scattering. The calculation presented here is less elaborate than previous methods of assessing these multiparton interactions [7–9], but it has the advantage of being constrained by a recent measurement of the double parton interaction rate [10].

In view of the importance of the inclusive jet cross section, it is urgent to settle the question of underlying event level definitively. This can be done by measuring it as described in Sec. III. The measurement will also serve as a test of the assumptions used to make the estimate, which involve interesting unexplored areas of non-perturbative QCD.

We have focused on  $E_T$  in an  $R = 0.7$  cone, because that is the relevant quantity for estimating the incoherent background under a jet. The background will also have an important influence on “jet shape” observables such as the cone

size dependence  $\psi(r) = \sum_{r_i < r} E_T^i / \sum_{r_i < R} E_T^i$  [19]. To study the underlying event mechanism in more detail, it would be useful to apply the technique based on Marchesini and Webber [16] that is discussed in Sec. III using regions of different sizes as well. It would also be useful to apply the technique to different hard processes such as  $W$  and  $W + 1$  jet production, and for comparison to minimum bias events.

## ACKNOWLEDGMENTS

I thank J. Huston and W.K. Tung for comments on the manuscript, and H.L. Lai for supplying numerical values for the CTEQ4M inclusive jet prediction. This work was supported in part by U.S. National Science Foundation grant number PHY-9507683.

- 
- [1] CDF Collaboration, F. Abe *et al.*, Phys. Rev. Lett. **77**, 438 (1996).
- [2] D0 Collaboration, G. C. Blazey, Proceedings of the 31st Rencontres de Moriond: QCD and High-Energy Hadronic Interactions, Les Arcs, France (1996), p. 155; CDF and D0 Collaborations, Freedy Nang, FERMILAB-CONF-97-192-E.
- [3] H. L. Lai, J. Huston, S. Kuhlmann, F. Olness, J. Owens, D. Soper, W. K. Tung, and H. Weerts, Phys. Rev. D **55**, 1280 (1997); J. Huston, E. Kovacs, S. Kuhlmann, H. L. Lai, J. F. Owens, D. Soper, and W. K. Tung, Phys. Rev. Lett. **77**, 444 (1996).
- [4] D. Kosower, "Extracting Parton Densities from Collider Data," hep-ph/9708392.
- [5] G. Abbiendi, I. G. Knowles, G. Marchesini, B. R. Webber, M. H. Seymour, and L. Stanco, Comput. Phys. Commun. **67**, 465 (1992).
- [6] J. D. Bjorken, Phys. Rev. D **47**, 101 (1993); E. Gotsman, E. M. Levin, and U. Maor, Phys. Lett. B **309**, 199 (1993); CDF Collaboration, F. Abe *et al.*, Phys. Rev. Lett. **74**, 855 (1995); D0 Collaboration, S. Abachi *et al.*, *ibid.* **76**, 734 (1996).
- [7] T. Sjöstrand and M. van Zijl, Phys. Rev. D **36**, 2019 (1987).
- [8] Xin-Nian Wang and Miklos Gyulassy, Phys. Lett. B **282**, 466 (1992).
- [9] J. M. Butterworth, J. R. Forshaw, and M. H. Seymour, Z. Phys. C **72**, 637 (1996); J. M. Butterworth, J. R. Forshaw, and T. Sjöstrand, J. Phys. G **22**, 883 (1996); Miklos Gyulassy and Xin-Nian Wang, Comput. Phys. Commun. **83**, 307 (1994).
- [10] CDF Collaboration, F. Abe *et al.*, Phys. Rev. Lett. **79**, 584 (1997) and FERMILAB-PUB-97-094-E.
- [11] CDF Collaboration, F. Abe *et al.*, Phys. Rev. D **50**, 5550 (1994).
- [12] G. Schuler and T. Sjöstrand, Nucl. Phys. **B407**, 539 (1993).
- [13] M. Drees and T. Han, Phys. Rev. Lett. **77**, 4142 (1996).
- [14] T. Sjöstrand, hep-ph/9508391; T. Sjöstrand, Comput. Phys. Commun. **82**, 74 (1994).
- [15] J. D. Bjorken, "Collisions of constituent quarks at collider energies," SLAC-PUB-95-6949, in Lake Louise 1995, *Quarks and colliders*, p. 61; Acta Phys. Pol. B **23**, 637 (1992); S. Scopetta, V. Vento, and M. Traini, "Towards a unified picture of constituent and current quarks," hep-ph/9708262.
- [16] G. Marchesini and B. R. Webber, Phys. Rev. D **38**, 3419 (1988).
- [17] UA5 Collaboration, G. Alner *et al.*, Phys. Rep. **154**, 247 (1987).
- [18] D. E. Soper, "Jet observables in theory and reality," hep-ph/9706320.
- [19] M. H. Seymour, "Jet shapes in hadron collisions: higher orders, resummation and hadronization," Rutherford Lab Report No. RAL-TR-97-026, hep-ph/9707338; W. T. Giele, E. W. N. Glover, and David A. Kosower, Phys. Rev. D **57**, 1878 (1998).